



Extended architectures constructed of thiourea-modified SBA-15 nanoreactor: A versatile new support for the fabrication of palladium pre-catalyst

Hassan Alamgholiloo^{1,2} | Sadegh Rostamnia¹ | Nader Noroozi Pesyan²

¹Organic and Nano Group (ONG), Department of Chemistry, Faculty of Science, University of Maragheh, PO Box 55181-83111, Maragheh, Iran

²Department of Organic Chemistry, Faculty of Chemistry, Urmia University, 57159 Urmia, Iran

Correspondence

Sadegh Rostamnia, Organic and Nano Group (ONG), Department of Chemistry, Faculty of Science, University of Maragheh, PO Box 55181-83111, Maragheh, Iran.

Email: rostamnia@maragheh.ac.ir,
srostamnia@gmail.com

Nader Noroozi Pesyan, Department of Organic Chemistry, Faculty of Chemistry, Urmia University, 57159 Urmia, Iran.

Email: nnp403@gmail.com

We designed and synthesized a novel catalyst consisting of ordered mesoporous silica (SBA-15) functionalized with bis(thiourea) (BTU) linker. The regular and unique pore channels of BTU-SBA-15 ensure proper control of the size and homogeneous distribution of palladium nanoparticles. The physicochemical properties of the hybrid Pd@BTU-SBA-15 pre-catalyst were investigated using various techniques. The proposed catalyst is found to be very active, reusable, stable and scalable, and has excellent reactivity and selectivity for Suzuki and Heck coupling reactions under very mild and sustainable reaction conditions.

KEY WORDS

C–C coupling reaction, heterogeneous catalysisordered mesoporous silicaPd@BTU-SBA-15

1 | INTRODUCTION

Within the field of mesoscale nanoarchitecturing,^[1] ordered mesoporous silica (OMS) including the family of MCM and SBA has attracted increased interest in recent years because of its unique properties including narrow pore distribution, high loading and adjustable pore diameter.^[2,3] Because of these properties, numerous applications of these nanoreactors in different fields have been explored including sensing,^[4,5] chromatography,^[6] drug delivery,^[7,8] energy storage^[9,10] and catalysis.^[11–14] Recently, an enormous research effort has been made into the modification of OMS with noble metal nanoparticles. Incorporation of noble metals such as gold, palladium and platinum into OMS has been explored via methods such as impregnation,^[15] deposition–precipitation,^[16] vacuum calcination,^[17] hybrid grafting,^[18] colloid immobilization,^[19] etc.

Palladium nanoparticles (Pd NPs) have been immobilized on a wide range of solid materials and

have been applied as efficient catalysts for many reactions such as cross-coupling, domino reactions, dehydrogenation/hydrogenation, oxidation and reduction, and others. Among carbon–carbon coupling reactions, the Suzuki and Heck reactions due to mild reaction conditions, insensitivity to moisture, tolerance of active functional groups and low toxicity are the most explored examples.^[20–23] Numerous investigations have indicated that supports with functional groups such as amines,^[24] imines,^[25] thiols,^[2] phosphine^[26] and sulfonic acids^[27] could be anchored on the surface of silica materials and then interacted with Pd NPs for use in coupling reactions. Very recently, our research group has explored several silica materials and PMO-type hybrid support for encapsulation of transition metal nanoparticles and organic functional groups for catalytic aims.^[14,28,29]

In the work reported here, uniform Pd NPs were synthesized on SBA-15 mesoporous silica and modified with bis(thiourea) (BTU) ligand. Good affinity between

the BTU ligand and the template walls is vitally important for anchoring and stabilizing the Pd NPs. Finally, we found that BTU-SBA-15 is not only a superb scavenger for Pd NPs, but also for both Suzuki and Heck reactions, there is negligible leaching of Pd into solution.

2 | EXPERIMENTAL

2.1 | Characterization

The mesoporous material was characterized using powder X-ray diffraction (XRD) measurements (Philips-PW 1800 diffractometer). Scanning electron microscopy (SEM) images were recorded with a Hitachi S-4800 field emission scanning electron microscope. Transmission electron microscopy (TEM) and elemental mapping images were obtained using a JEM-2100F with an accelerating voltage of 200 kV. The electronic state of metal present in samples was determined using X-ray photoelectron spectroscopy (XPS). Fourier transform infrared (FT-IR) spectra were obtained using a Shimadzu IR-640 spectrometer. Nitrogen adsorption–desorption isotherms were measured at 77 K with a Quantachrome Autosorb, from which the specific surface area (S_{BET}) and the average pore diameter (D_p) were calculated using the multiple-point Brunauer–Emmett–Teller method. ^1H NMR and ^{13}C NMR spectra were recorded with a Bruker Avance 300 spectrometer. The Pd loading was determined using inductively coupled plasma atomic emission spectroscopy (ICP-AES) with a PerkinElmer 2100DV.

2.2 | Fabrication of BTU ligand

The synthesis of the BTU ligand (N,N' -bis(3triethoxysilylpropyl)) was performed following our previously reported methodology with modifications.^[30] Typically, carbon disulfide (CS_2 ; 10 mmol, 600 μl) and 3-aminopropyltriethoxysilane (APTES; 20 mmol, 4.68 ml) were added to a two-necked 20 ml glass balloon under inert atmosphere. Then, the temperature was raised

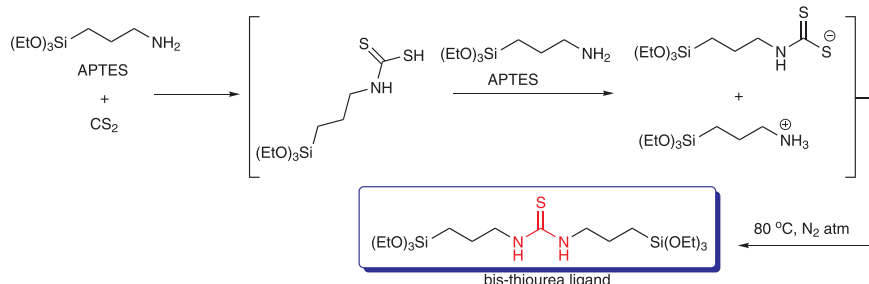
slowly to 353°C for 2 hours. A change in the color and evolution of hydrogen sulfide (H_2S) gas from the mixture showed completion of the synthesis process. Finally, the reaction was allowed to cool to ambient conditions and the final product in 78.5% yield was obtained (Scheme 1 and supporting information).

2.3 | Synthesis of BTU-SBA-15

The mesoporous material was synthesized based on our previous reports of the synthesis of SBA-15 with slight modifications.^[31,32] An amount of 1.0 g of calcined SBA-15 was dispersed in 25 ml of toluene under an inert atmosphere. A mixture of the BTU ligand prepared as described above (5.0 mmol, 2.42 ml) was added dropwise to the reaction. Then, the temperature was raised to 383 K and allowed to stir for 12 hours under an inert atmosphere. To remove residual unreacted ligand, the synthesized BTU-SBA-15 was purified with absolute EtOH and CH_2Cl_2 several times, and finally it was filtered and dried at 353 K during 12 hours. The loading of BTU ligand in the nanoreactor structure was approximately 54% as measured using elemental analysis with energy-dispersive X-ray spectroscopy (EDS).

2.4 | Preparation of Pd@BTU-SBA-15

PdCl_2 (20 mg) and poly(vinyl alcohol) (PVA; PVA monomer-to- PdCl_2 molar ratio = 9:1) were mixed in 50 ml of deionized water and then was stirred for 1 hour at 273 K. Then, 20 ml of 0.1 M NaBH_4 was added dropwise to the mixture to fabricate a colloidal Pd solution. Finally, 0.50 g of BTU-SBA-15 prepared as described above was added to the solution. The mixture reaction was stirred for 6 hours under ambient conditions. The Pd@BTU-SBA-15 was filtered and washed several times with EtOH and CH_2Cl_2 and dried at 373 K overnight. The amount of palladium in Pd@BTU-SBA-15 was 3.04 wt% as measured using atomic absorption spectrometry (AAS).



S C H E M E 1 Procedure for preparation of BTU linker

2.5 | Catalysis with Pd@BTU-SBA-15 (Suzuki and Heck coupling reactions)

The Suzuki reaction was carried out under ambient conditions in a 20 ml Schlenk tube containing 1 mmol of aryl halide, 1.1 mmol of arylboronic acid, 2 mmol of K_2CO_3 and Pd@BTU-SBA-15 (0.30 mol%) in 5 ml of deionized water. The resultant mixture was stirred at room temperature for 2 hours, diluted with absolute EtOH and centrifuged. 1H NMR and ^{13}C NMR spectroscopy was used to identify the main product. For the Heck reaction, 1 mmol of aryl halide and 1.2 mmol of alkene were added to a mixture of 2 mmol of K_2CO_3 and Pd@BTU-SBA-15 catalyst (0.25 mol%) in 5 ml of dimethylformamide (DMF)– H_2O (1: 1 v/v). The resultant mixture was refluxed at 120°C for 12 hours. Finally, desired product was extracted followed by analysis according to the method described above. To determine the catalyst durability for both Suzuki and Heck reactions, the Pd pre-catalyst was centrifuged after each cycle of the reactions. The Pd catalyst was washed thoroughly with absolute EtOH and CH_2Cl_2 , followed by drying at 373 K under vacuum condition.

3 | RESULTS AND DISCUSSION

In the present study, we designed BTU-functionalized SBA-15 for immobilization of ultrafine Pd NPs. In fact, we demonstrate a facile preparation method for the synthesis of three-dimensional OMS with Pd NPs loaded on both external and internal channels of the mesopores. By embedding the organic ligands within the pore walls, the hydrophobic–hydrophilic properties of the nanoreactor are well controlled. A schematic illustration of the synthesis of Pd@BTU-SBA-15 is shown in Figure 1. Also, the

thiourea ligand and pore structure of the nanoreactor play an important role in the good control of the Pd metal size and homogeneous dispersion, thus enhancing the catalytic activity for both Suzuki and Heck reactions.

To verify this speculation, FT-IR analysis was utilized to explore the chemical structure of SBA-15, BTU-SBA-15 and Pd@BTU-SBA-15. As illustrated in Figure 2a, a broad and small band at 3241 cm^{-1} corresponded to N&bond;H stretching. The spectra also contain strong absorption bands at 2920 and 2852 cm^{-1} which can be ascribed to the symmetric and asymmetric stretching mode of aliphatic C&bond;H bonds, respectively.^[14,33–35] A new peak appears at 936 cm^{-1} corresponding to C&bond;N bond, suggesting the successful preparation of BTU-SBA-15. The porous structure of the resulting materials was confirmed using nitrogen adsorption–desorption isotherm measurements. As shown in Figure 2b, the isotherm is a type IV curve with a hysteresis loop in the relative pressure range 0.45–0.9, which demonstrates a mesoporous structure. As presented in Figure 2b, immobilization Pd@thiourea into the pore cage of SBA-15 is evidenced with a simultaneous decrease of the mesoporous surface area from 670 $cm^2 g^{-1}$ for SBA-15 to 286 $cm^2 g^{-1}$ for Pd@BTU-SBA-15. As calculated using the Barrett–Joyner–Halenda method, the pore diameters for native SBA-15 and Pd@BTU-SBA-15 were 6.8 and 4.3 nm, respectively. The small-angle XRD pattern for nanoreactor SBA-15 shows one sharp peak at $2\theta = 0.94^\circ$, the peak positions matching well with the simulated diffraction pattern.^[36,37] After BTU ligand immobilization, this peak was maintained and slightly shifted to $2\theta = 0.98^\circ$, which originates from the periodicity of the nanoreactor structure. A comparison of the XRD pattern of Pd@BTU-SBA-15 with that of SBA-15 revealed a shift to higher 2θ angles, although other main diffraction peaks showed some slight decreases of peak

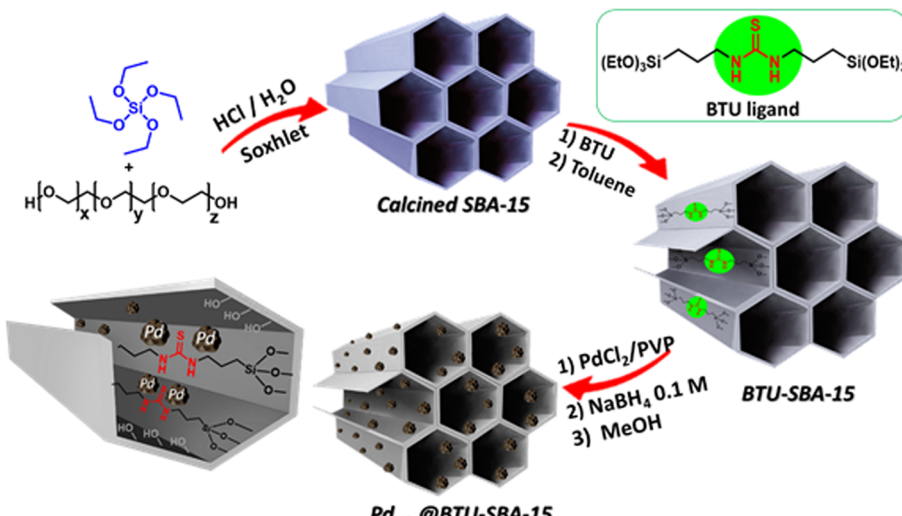


FIGURE 1 General pathway for preparation of Pd@BTU-SBA-15

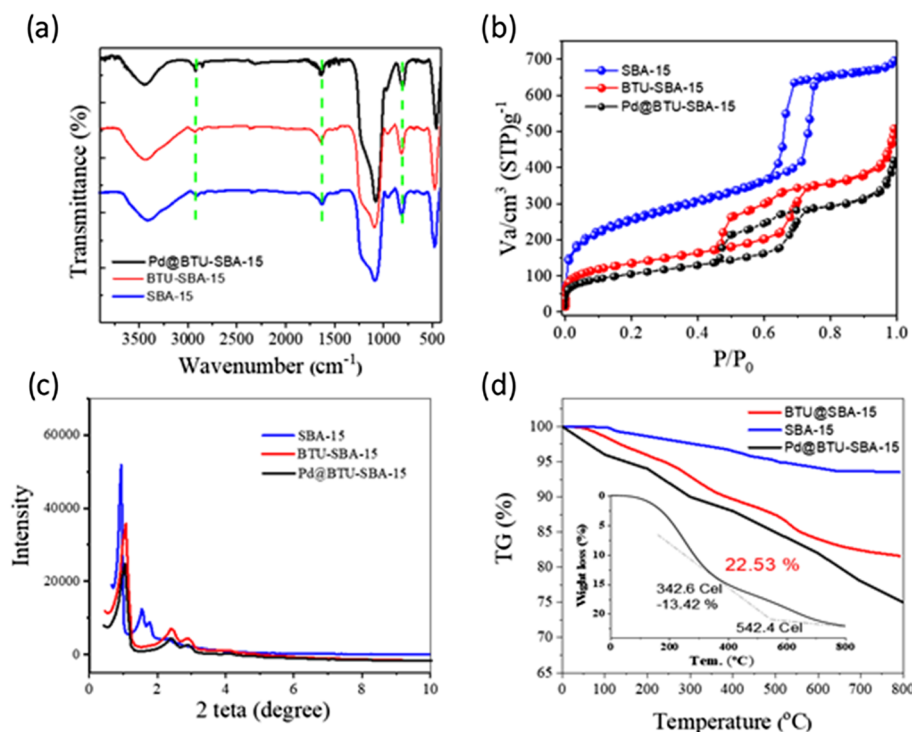


FIGURE 2 (a) FT-IR spectra of SBA-15 and Pd@BTU-SBA-15. (b) Nitrogen adsorption-desorption profiles of SBA-15, BTU-SBA-15 and Pd@BTU-SBA-15. (c) Small-angle XRD patterns of SBA-15, BTU-SBA-15 and Pd@BTU-SBA-15. (d) TGA of Pd@BTU-SBA-15

intensities with the immobilization of Pd NPs, due to the partial filling by the grafting guest molecules. To estimate the ratio of the organic moiety to silica in the Pd@BTU-SBA-15 structure, thermogravimetric analysis (TGA) was conducted (Figure 2d). Based on the TGA, the pure SBA-15 nanoreactor had a 5.11% weight loss at temperatures up to 800°C, which was attributed to the loss from the surface decomposition of silanol groups and a small amount of adsorbed water. In the case of BTU@SBA-15 and Pd@BTU-SBA-15, the weight losses were 17.36 and 22.53 wt%, respectively, due to the decomposition of small-molecule functionalized organic matter.

The electronic states of metallic Pd particles in Pd@BTU-SBA-15 were identified through XPS analysis (Figure 3). The XPS spectrum of the Pd (3d) core levels shows two intense photopeaks with maximum binding energy values of 337.2 and 342.5 eV ascribed to the Pd 3d_{5/2} and 3d_{3/2} doublet, respectively. These binding energy values are consistent with the presence of palladium species in the metallic state and are in agreement with the theoretical value.^[38–42] Therefore, these analyses demonstrate that immobilized Pd NPs were thoroughly reduced in the nanoreactor structure.

The morphology of the obtained mesostructure was investigated through SEM and TEM, and the elemental composition studied using EDS as shown in Figure 4. SEM images exhibit the rod-like morphology of BTU-SBA-15 and even Pd growth in surface mesopores (Figure 4a,d). But after the deposition of Pd NPs, the

SBA-15 morphology barely shows the Pd NPs inside and outside of the SBA-15 pores. The TEM images can provide more detailed information that enables one to observe the presence of porosity and Pd NPs on BTU-SBA-15 (Figure 4c,f). As shown in Figure 4d, the Pd NPs in Pd@BTU-SBA-15d was found to be ultra-small, having an average size ranging from 1.8 to 4 nm. When only SBA-15 was utilized instead of the BTU-functionalized SBA-15 for the deposition of Pd NPs, particle sizes of greater than 5.5 nm in the nanoreactor were found.^[43,44] Also, SEM-EDS analysis was performed for the mesoporous materials. Based on this

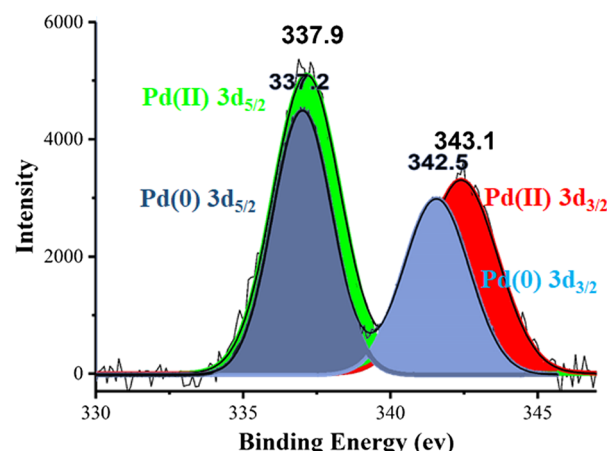


FIGURE 3 XPS pattern of Pd@BTU-SBA-15

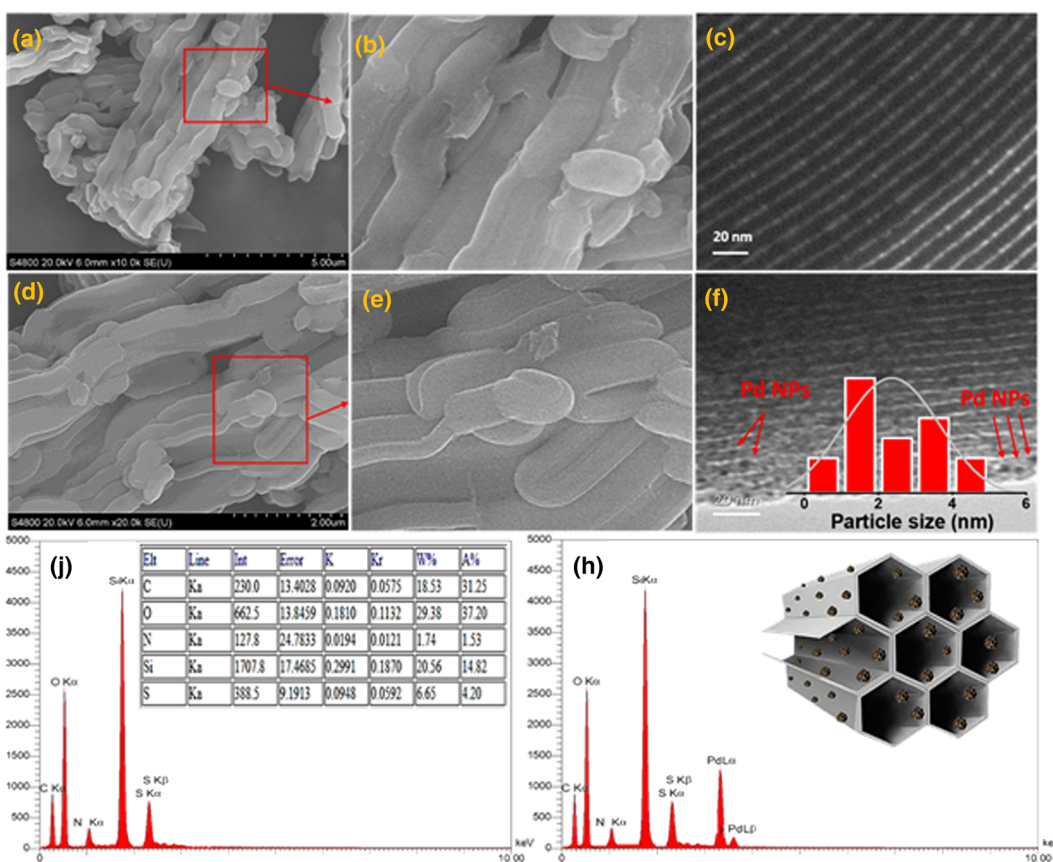


FIGURE 4 (a) SEM and (c) TEM images of BTU-SBA-15. (d) SEM and (f) TEM images of Pd@TU-SBA-15. (b, e) magnified SEM images of BTU-SBA-15 and Pd@BTU-SBA-15. (j, h) EDS analysis of BTU-SBA-15 and Pd@BTU-SBA-15

analysis, palladium, sulfur and nitrogen atoms are present in the structure of Pd@BTU-SBA-15 which exhibits purity and successful deposition of Pd to SBA-15. The

amount of Pd in the mesoporous material structure was determined using AAS. According to this, the amount of Pd was 3.04 wt%.

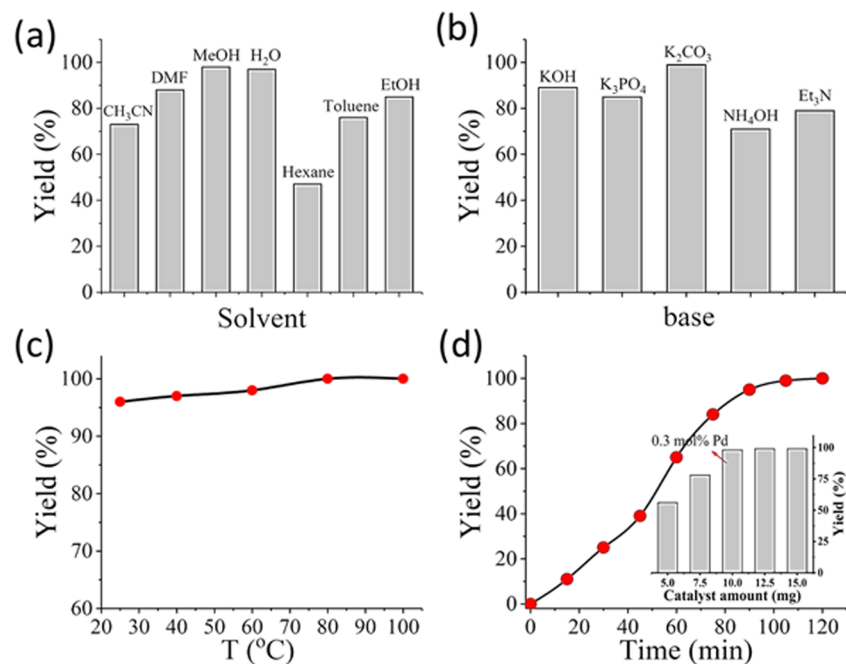


FIGURE 5 (a) Reaction progress in various solvents under similar conditions. (b) Base effect under optimized conditions for Suzuki reaction catalyzed by Pd@BTU-SBA-15 at room temperature. (c) Effect of temperature on progress of Suzuki coupling reaction. (d) Kinetic study and effect of amount of catalyst on progress of Suzuki coupling reaction

TABLE 1 Substrate scope for Suzuki coupling^a

Entry	Ar	Hal	R	Conversion (%)	Yield (%) ^b
1	Ph	I	H	>99(89) ^c	98(87)
2	Ph	I	<i>p</i> -Me	98	97
3	<i>p</i> -Me-Ph	I	H	>99	98
4	<i>o</i> -Me-Ph	I	H	98	96
5	<i>p</i> -MeO-Ph	I	H	98	97
6	<i>p</i> -MeO-Ph	I	<i>m</i> -Me	97	96
7	<i>o</i> -MeO-Ph	I	H	98	97
8	<i>o</i> -MeO-Ph	I	<i>m</i> -Me	93	95
9	<i>p</i> -MeCO-Ph	I	H	99	98
10	<i>p</i> -MeCO-Ph	I	<i>m</i> -Me	98	98
11	<i>m</i> -NO ₂ -Ph	I	H	97	96
12	Ph	Br	H	97(87)	96(86)
13	<i>o</i> -MeO-Ph	Br	<i>m</i> -Me	95	88
14	<i>m</i> -CHO-Ph	Br	H	90	87
15	<i>m</i> -NO ₂ -Ph	Br	<i>p</i> -Me	89	85
16	<i>p</i> -MeCO-Ph	Br	H	97	97
17	<i>p</i> -MeCO-Ph	Br	<i>m</i> -Me	96	95
18	<i>m</i> -CHO-Ph	Cl	H	66(51)	59(50)
19	<i>p</i> -MeCO-Ph	Cl	<i>m</i> -Me	78	69
20	Ph	F	<i>m</i> -Me	Trace	Trace
21	Ph	I	H	Trace ^d	Trace

^aReaction conditions: **1** (1.0 mmol), **2** (1.1 mmol), catalyst (0.3 mol% Pd), K₂CO₃ (2.0 mmol), deionized water (5 ml), 25°C.

^bIsolated yield.

^cPd(II)@BTU-SBA-15 was applied.

^dBTU-SBA-15 and SBA-15 were applied.

3.1 | Catalytic activity

3.1.1 | Suzuki coupling reaction

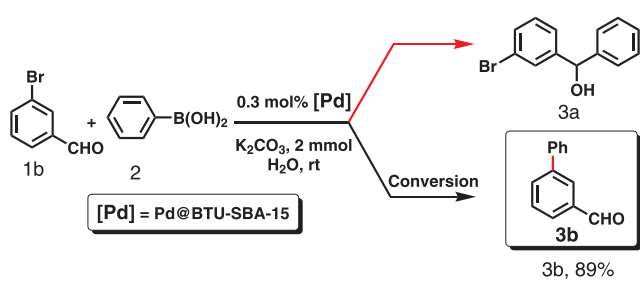
The Suzuki reaction is considered one of the most popular methods for forming C–C sp² bonds in modern synthesis. We initiated our study by examining the reaction of phenylboronic acid and *p*-bromoacetophenone as a model reaction for optimization of the reaction conditions (base, solvent, temperature and reaction time). Obviously, reaction in the absence of any Pd catalyst and base did not afford the desired product. Among a variety of bases that showed satisfactory results such as K₂CO₃, KOH, K₃PO₄, NH₄OH and Et₃N, we chose to proceed with K₂CO₃

because it afforded the highest conversion (Figure 5b). When we studied the reaction progress with various solvents including EtOH, MeOH, DMF, CH₃CN, hexane, toluene and water, we found that MeOH and water affording 99% conversion are more efficient than the other solvents (Figure 5a). Our interest was in using water to replace organic solvents in such reactions because water solvent endows the reaction with green character, and is readily available, of low cost and safe.^[45] In EtOH, MeOH, DMF and CH₃CN, the catalyst system afforded the corresponding coupling product in moderate yields; however, hexane was found to be a poor solvent for the same process. Despite increasing the reaction conversion by increasing the temperature, based on the importance of room

temperature in chemical processes and for energy issues, we continued our studies under ambient conditions (Figure 5c). Finally, we noted that the reaction progress was initially slow and then the rate of reaction increased until completion at 2 hours (Figure 5d). We also screened the amount of supported Pd catalyst, and 0.30 mol% loading of Pd in Pd@BTU-SBA-15 was found to be optimal (Figure 5d, inset).

To gain further insights into the generality and limitations of the catalytic system in the Suzuki coupling reaction, we extended our studies to various types of aryl halides and phenylboronic acid derivatives (Table 1). A variety of aryl halides and phenylboronic acids were readily coupled to afford the desired product in excellent conversion without homocoupling.

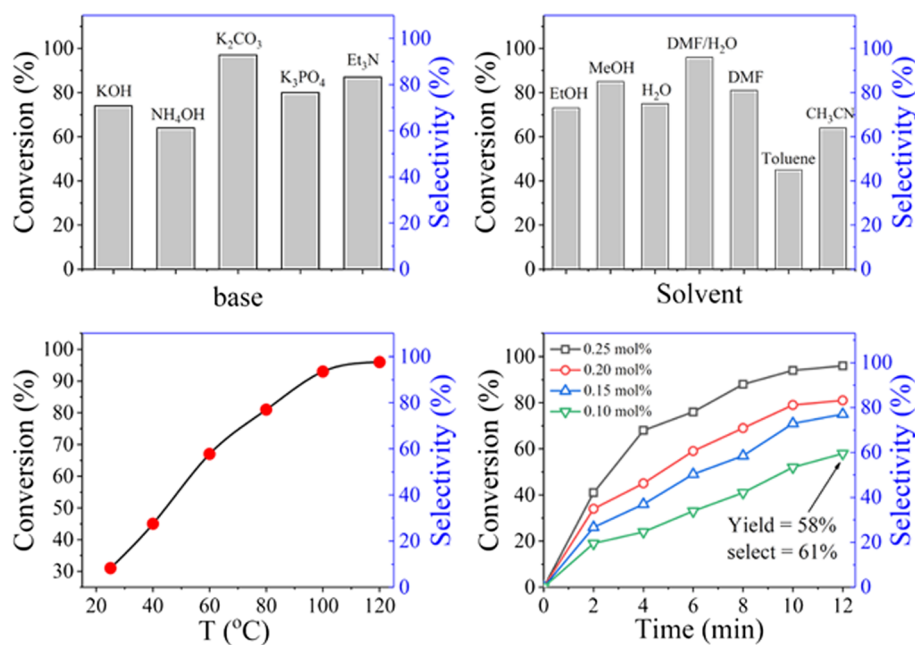
After finding that the Pd catalyst was compatible with aryl halides and phenylboronic acid, investigation was undertaken of the chemoselectivity with the reaction of phenylboronic acid and *m*-bromobenzaldehyde. Under



the optimized conditions, the reaction of **1b** and **2** for 2 hours gave biaryl product **3b** in a yield of 89% and corresponding benzophenone derivative **3a** was not observed (Scheme 2). The present result indicates the chemoselectivity Pd@BTU-SBA-15.

3.1.2 | Heck coupling reaction

Due to the promising results for Suzuki coupling, we became interested in testing the Pd catalytic system in the Heck coupling reaction. We found that Pd@BTU-SBA-15 was very active for the Heck reaction of a variety of aliphatic and aromatic alkenes with aryl halides. First, the coupling of iodobenzene with methyl acrylate was chosen as a model reaction. In a preliminary experiment, it was found that K₂CO₃ afforded the best conversion in comparison with other bases such as KOH, K₃PO₄, NH₄OH and Et₃N (Figure 6a). Due to the low cost and high conversion, K₂CO₃ was chosen as a base for this coupling reaction. In the next step, the influence of the solvent on the catalytic activity was investigated. The catalytic performance in DMF-H₂O (1:1 v/v) was higher than that in water, DMF and other polar/nonpolar solvents. In addition, toluene was found to be a poor solvent for the same process (Figure 6b). Increasing the temperature to reflux condition (120°C) improved the conversion of the reaction slightly to 97% (Figure 6c). By increasing the amount of the catalyst from 10 to 25 mg, conversion and selectivity of the reaction were also increased (Figure 6d). From the results shown in Figure 6d,



when the amount of Pd catalyst was reduced to 0.10 mol%, the yield and selectivity decreased to 58% and 61%.

Considering the promising results obtained, as described above, we were interested in demonstrating the usefulness of the developed catalytic system for other substrates. As presented in Table 2, aryl iodides compared to aryl bromides and aryl chlorides gave a high conversion in a short reaction time. We found that using Pd@BTU-SBA-15 the Heck reaction between aryl halides and alkenes proceeded with a low amount of catalyst loading under sustainable and environmentally benign conditions.

Among various Pd-based catalysts, the proposed pre-catalyst afforded excellent yield and selectivity for both coupling reactions, superior to that of most of the reported catalysts (Table 3). However, yield is lower than that for Pd(II)-doped UiO-67,^[50] Pd/ED-MIL-101^[54] and homogeneous catalysts. The results demonstrate the strong effects of the BTU ligand in comparison with other

ligands for stabilizing and keeping the Pd NPs in an active state in the SBA-15 structure.

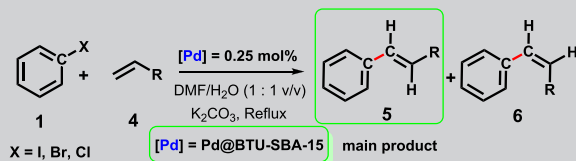
3.2 | Heterogeneity studies

In order to reach a deeper understanding of whether or not the proposed catalyst is heterogeneous in nature, we performed a series of control experiments such as those involving ICP-AES analysis and hot filtration. ICP-AES analysis of both coupling reactions indicated that negligible Pd leaching occurred (detection limit of 0.7–10 ppm). The hot filtration test of the reaction suspension with removal of the insoluble Pd@BTU-SBA-15 also led to the inhibition of both Suzuki and Heck reactions (Figure 7). ICP-AES analysis and the hot filtration test confirmed that the proposed catalyst is truly heterogeneous in nature.

Taking into account the above observations and the mechanism for Suzuki and Heck coupling reactions

TABLE 2 Substrate scope for Heck coupling^a

Entry	Ar	Hal	R	Conversion (%) ^b	Selectivity (%) ^c
1	p-Me-Ph	I	Ph	97(90) ^d	98(96)
2	p-Me-Ph	I	CO ₂ Me	96	98
3	p-OMe-Ph	I	Ph	94	97
4	p-OMe-Ph	I	CN	97	98
5	m-NO ₂ -Ph	I	CN	94	94
6	m-NO ₂ -Ph	I	CO ₂ Et	92	94
7	Ph	Br	CO ₂ Me	91(82)	98(96)
8	Ph	Br	CO ₂ Et	90	98
9	Ph	Br	CO ₂ Bt	88	97
10	p-COMe-Ph	Br	CO ₂ Me	92	98
11	p-COMe-Ph	Br	CO ₂ Et	91	97
12	m-CHO-Ph	Cl	CO ₂ Me	64(43)	95(94)
13	p-MeCO-Ph	Cl	CO ₂ Et	69	95
14	p-Me-Ph	I	Ph	Trace ^e	Trace



^aReaction conditions: **1** (1.0 mmol), **4** (1.2 mmol), catalyst (0.25 mol% Pd), K₂CO₃ (2.0 mmol), DMF–H₂O (1:1 v/v, 5 mL), 120 °C.

^bConversion determined by TLC.

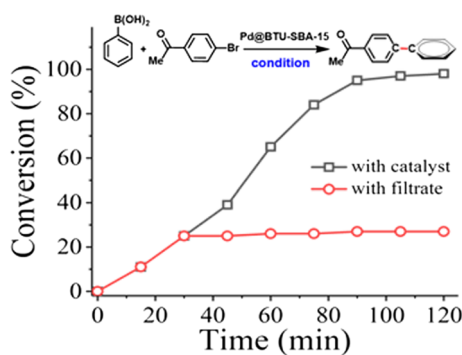
^cSelectivity to *trans*-alkene.

^dPd(II)@BTU-SBA-15 was applied.

^eBTU-SBA-15 and SBA-15 were applied.

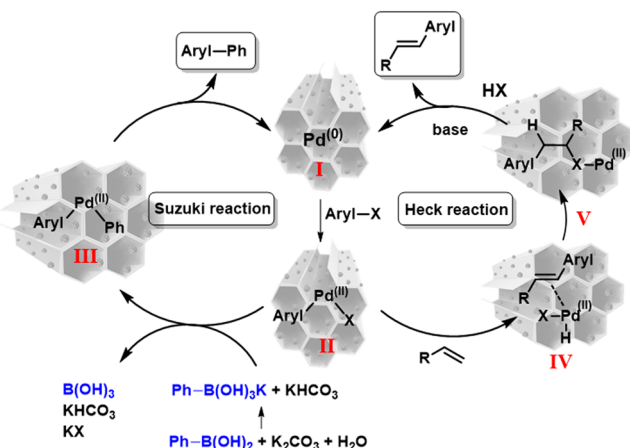
TABLE 3 Comparison of catalytic activity of various catalysts for Suzuki and Heck coupling

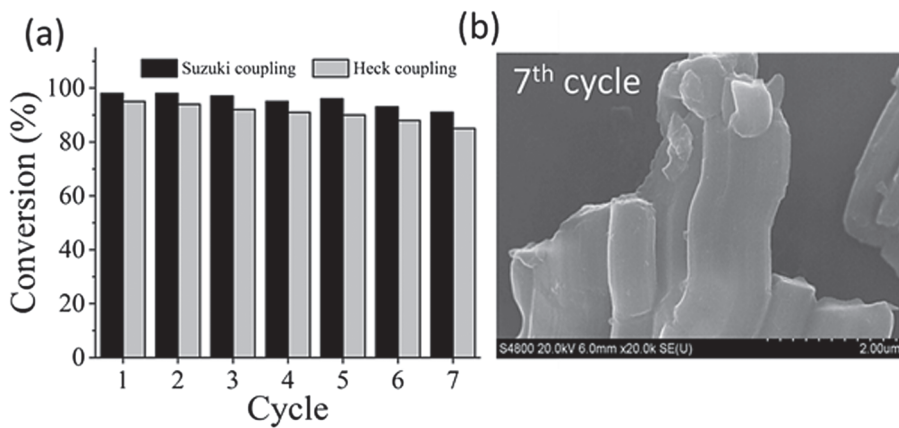
Reaction	Catalyst	Reaction conditions	Yield (%)	Ref.
Suzuki reaction	Pd@SBA-15(SH) ₂	K ₂ CO ₃ , H ₂ O, 80°C	98	[32]
	Pd@BTU-PMO	K ₂ CO ₃ , H ₂ O, 25°C	95	[14]
	Pd-PPPh ₂ -SBA-15	K ₂ CO ₃ , isopropanol, 80°C	97	[46]
	Pd(0)/MCoS-1	K ₂ CO ₃ , H ₂ O, 70°C	96	[47]
	Pd@CuBDC/Py-SI	K ₂ CO ₃ , DMF/H ₂ O, 80°C	98	[48]
	m-MCFSH-Pd	EtOH, Na ₃ PO ₄ , 60°C	80	[2]
Heck reaction	Pd@BTU-SBA-15	K ₂ CO ₃ , H ₂ O, 25°C	98	This study
	Fe ₃ O ₄ @SiO ₂ /Schiff base/Pd ^{II}	K ₂ CO ₃ , DMF, 110°C	97	[49]
	Pd(II)-doped UiO-67	K ₂ CO ₃ , DMF, TBAB, 100°C	97	[50]
	Pd ^{II} @Cu (BDC)/2-Py-SI	K ₂ CO ₃ , DMF, 120°C	98	[51]
	(PdCl ₂ /bpy) ₁₀ multilayers	Na ₂ CO ₃ , DMF, 140°C	95	[52]
	Pd/ED-MIL-101	Et ₃ N, DMF, 120°C	98	[53]
Heck reaction	Pd-PPPh ₂ -SBA-15	Et ₃ N, NMP, 80°C	90	[46]
	Pd@BTU-SBA-15	K ₂ CO ₃ , DMF/H ₂ O, 120°C	96	This study

**FIGURE 7** Activity profile for Suzuki reaction. Reaction conditions: 4-bromoacetophenone (1 mmol), phenylboronic acid (1.1 mmol) containing 3 mol% Pd@BTU-SBA-15 in 5 ml of water, at room temperature

previously reported,^[55,56] a plausible catalyst cycle is proposed in Scheme 3. For the Suzuki reaction, the *oxidative addition* of aryl halides to zero-valent Pd immobilized in BTU-SBA-15 is the initial step to give divalent Pd species and intermediate **II**. With the participation of base (K₂CO₃), an organoborane reacts with intermediate **II** in *transmetalation* to afford intermediate **III**. Finally, reductive elimination gives the desired product and regenerates the active zero-valent Pd in the nanoreactor. In the Heck reaction, a different catalytic cycle involves coupling between aryl halides and olefins. In the first step, the olefin is coordinated to intermediate **II** and then a *syn* insertion occurs. Intermediate **V** formed in the previous step, undergoes β-hydride elimination to form the *trans*-alkene product. Finally, a base (K₂CO₃) removes H&bond;X to regenerate the zero-valent Pd species in the BTU/SBA-15 structure.

Finally, in order to determine the activities and stabilities of Pd@SBA-15 for repeat runs, reusability experiments were also performed in both Suzuki and Heck reactions under optimal conditions. The results shown in Figure 8a indicate that proposed catalyst could be recycled for both reactions in up to seven successive runs. However, a small decrease of yield was observed after each reaction cycle which could be ascribed to the fact that a small fraction of the catalyst is lost in each recovery. This indicated that the Pd immobilized in BTU-SBA-15 was robust and recyclable. According to AAS analysis, negligible Pd was detected in the reaction solution up to the seventh run, and SEM imaging revealed the formidable stability of the catalyst under the investigated reaction conditions even after the seventh run (Figure 8b).

**SCHEME 3** Possible mechanism of Suzuki and Heck reactions using Pd@BTU-SBA-15



4 | CONCLUSIONS

We have demonstrated the syntheses of SBA-15 nanoreactor and its BTU-grafted counterpart as an excellent support for stabilizing ultrafine Pd NPs. Then, Suzuki and Heck coupling reactions were separately addressed via immobilization of uniform Pd NPs into of the SBA-15 support under very mild and sustainable reaction conditions. Excellent recycling capacities of the catalytic system were also assessed for up to seven consecutive recycles with negligible leaching of Pd NPs from the Pd@BTU-SBA-15 pre-catalyst. We believe that this method is quite simple, with environmental and economic benefits of the precursor, and it is anticipated that the strategy can be extended for the synthesis of other silica-based systems. By modifying these nanoreactors with various other organic ligands and noble metal nanoparticles, the application possibilities could be extended to a wide range including energy storage, dehydrogenation of HCOOH, conversion and organic transformations including hydrogenations, C&bond;X (X = C, O and N) bond forming reactions, and beyond.

ORCID

Sadegh Rostamnia <https://orcid.org/0000-0001-6310-8754>

Nader Noroozi Pesyan <https://orcid.org/0000-0002-4257-434X>

REFERENCES

- R. R. Salunkhe, Y. V. Kaneti, J. Kim, J. H. Kim, Y. Yamauchi, *Acc. Chem. Res.* **2016**, *49*, 2796.
- R. L. Oliveira, W. He, R. J. K. Gebbink, K. P. de Jong, *Catal. Sci. Technol.* **2015**, *5*, 1919.
- H. Batmani, N. Noroozi Pesyan, F. Havasi, *Appl. Organometal. Chem.* **2018**, *32*, e4419.
- L.-L. Li, H. Sun, C.-J. Fang, J. Xu, J.-Y. Jin, C.-H. Yan, *J. Mater. Chem.* **2007**, *17*, 4492.
- R. Métivier, I. Leray, B. Lebeau, B. Valeur, *J. Mater. Chem.* **2005**, *15*, 2965.
- X. Liu, L. Li, Y. Du, Z. Guo, T. T. Ong, Y. Chen, S. C. Ng, Y. Yang, *J. Chromatogr. A* **2009**, *1216*, 7767.
- I. I. Slowing, J. L. Vivero-Escoto, C.-W. Wu, V. S.-Y. Lin, *Adv. Drug Delivery Rev.* **2008**, *60*, 1278.
- M. Vallet-Regí, F. Balas, D. Arcos, *Angew. Chem. Int. Ed.* **2007**, *46*, 7548.
- J. Wang, M. Yang, Y. Lu, Z. Jin, L. Tan, H. Gao, S. Fan, W. Dong, G. Wang, *Nano Energy* **2016**, *19*, 78.
- S. Angioni, D. Villa, A. Cattaneo, P. Mustarelli, E. Quartarone, *J. Power Sources* **2015**, *294*, 347.
- J. Y. Ying, C. P. Mehnert, M. S. Wong, *Angew. Chem. Int. Ed.* **1999**, *38*, 56.
- H. G. Hosseini, S. Rostamnia, *New J. Chem.* **2018**, *42*, 619.
- H. G. Hosseini, E. Doustkhah, M. V. Kirillova, S. Rostamnia, G. Mahmoudi, A. M. Kirillov, *Appl. Catal. A* **2017**, *548*, 96.
- E. Doustkhah, S. Rostamnia, M. Imura, Y. Ide, S. Mohammadi, C. J. Hyland, J. You, N. Tsunoji, B. Zeynizadeh, Y. Yamauchi, *RSC Adv.* **2017**, *7*, 56306.
- A. K. Medina-Mendoza, M. A. Cortés-Jácome, J. A. Toledo-Antonio, C. Angeles-Chávez, E. López-Salinas, I. Cuauhtémoc-López, M. C. Barrera, J. Escobar, J. Navarrete, I. Hernández, *Appl. Catal. B* **2011**, *106*, 14.
- S. Chytil, W. R. Glomm, E. A. Blekkan, *Catal. Today* **2009**, *147*, 217.
- H.-C. Wu, T.-C. Chen, N.-C. Lai, C.-M. Yang, J.-H. Wu, Y.-C. Chen, J.-F. Lee, C.-S. Chen, *Nanoscale* **2015**, *7*, 16848.
- C.-m. Yang, P.-h. Liu, Y.-f. Ho, C.-y. Chiu, K.-j. Chao, *Chem. Mater.* **2003**, *15*, 275.
- W. Huang, J. N. Kuhn, C.-K. Tsung, Y. Zhang, S. E. Habas, P. Yang, G. A. Somorjai, *Nano Lett.* **2008**, *8*, 2027.
- B. Karimi, S. Abedi, J. H. Clark, V. Budarin, *Angew. Chem. Int. Ed.* **2006**, *45*, 4776.
- X. Zhang, H. Yin, J. Wang, L. Chang, Y. Gao, W. Liu, Z. Tang, *Nanoscale* **2013**, *5*, 8392.
- S. Rostamnia, T. Rahmani, *Appl. Organometal. Chem.* **2015**, *29*, 471.
- S. Rostamnia, T. Rahmani, H. Xin, *J. Ind. Eng. Chem.* **2015**, *32*, 218.
- P. Veerakumar, M. Velayudham, K.-L. Lu, S. Rajagopal, *Appl. Catal. A* **2013**, *455*, 247.
- C. Sarmah, D. Sahu, P. Das, *Catal. Today* **2012**, *198*, 197.
- D. Sahu, P. Das, *RSC Adv.* **2015**, *5*, 3512.

FIGURE 8 (a) Durability of catalyst in seven consecutive runs. (b) SEM image after seventh recycling of Pd@BTU-SBA-15

- [27] N. Oger, E. Le Grogne, F. X. Felpin, *ChemCatChem* **2015**, 7, 2085.
- [28] S. Rostamnia, E. Doustkhah, R. Bulgar, B. Zeynizadeh, *Micropor. Mesopor. Mater.* **2016**, 225, 272.
- [29] E. Doustkhah, S. Rostamnia, B. Zeynizadeh, J. Kim, Y. Yamauchi, Y. Ide, *Chem. Lett.* **2018**, 47, 1243.
- [30] E. Doustkhah, S. Rostamnia, N. Tsunoji, J. Henzie, T. Takei, Y. Yamauchi, Y. Ide, *Chem. Commun.* **2018**, 54, 4402.
- [31] D. Zhao, J. Feng, Q. Huo, N. Melosh, G. H. Fredrickson, B. F. Chmelka, G. D. Stucky, *Science* **1998**, 279, 548.
- [32] C. M. Crudden, M. Sateesh, R. Lewis, *J. Am. Chem. Soc.* **2005**, 127, 10045.
- [33] N. Mizoshita, M. Ikai, T. Tani, S. Inagaki, *J. Am. Chem. Soc.* **2009**, 131, 14225.
- [34] Y. Zhao, R. Jin, Y. Chou, Y. Li, J. Lin, G. Liu, *RSC Adv.* **2017**, 7, 22592.
- [35] Y. Niu, H. Liu, R. Qu, S. Liang, H. Chen, C. Sun, Y. Cui, *Ind. Eng. Chem. Res.* **2015**, 54, 1656.
- [36] T. E. Barder, S. D. Walker, J. R. Martinelli, S. L. Buchwald, *J. Am. Chem. Soc.* **2005**, 127, 4685.
- [37] X. Feng, G. Fryxell, L.-Q. Wang, A. Y. Kim, J. Liu, K. Kemner, *Science* **1997**, 276, 923.
- [38] C. J. Powell, *J. Electron Spectrosc. Relat. Phenom.* **2012**, 185, 1.
- [39] K. Koh, J.-E. Seo, J. Lee, A. Goswami, C. Yoon, T. Asefa, *J. Mater. Chem. A* **2014**, 2, 20444.
- [40] A. Lazar, C. Vinod, A. Singh, *Micropor. Mesopor. Mater.* **2017**, 242, 173.
- [41] A. Lazar, C. P. Vinod, A. P. Singh, *New J. Chem.* **2016**, 40, 2423.
- [42] A. F. Sierra-Salazar, A. Ayral, T. Chave, V. Hulea, S. I. Nikitenko, S. Abate, S. Perathoner, P. Lacroix-Desmazes, Unconventional pathways for designing silica-supported Pt and Pd catalysts with hierarchical porosity, in *Studies in Surface Science and Catalysis*, Netherlands: Elsevier **2019** 377.
- [43] D. Bhuyan, K. Selvaraj, L. Saikia, *Micropor. Mesopor. Mater.* **2017**, 241, 266.
- [44] Y. Duan, M. Zheng, D. Li, D. Deng, C. Wu, Y. Yang, *RSC Adv.* **2017**, 7, 3443.
- [45] Z. Guan, J. Hu, Y. Gu, H. Zhang, G. Li, T. Li, *Green Chem.* **2012**, 14, 1964.
- [46] J. Huang, M. Wang, S. Zhang, B. Hu, H. Li, *J. Phys. Chem. C* **2011**, 115, 22514.
- [47] A. S. Roy, J. Mondal, B. Banerjee, P. Mondal, A. Bhaumik, S. M. Islam, *Appl. Catal. A* **2014**, 469, 320.
- [48] S. Rostamnia, H. Alamgholiloo, X. Liu, *J. Colloid Interface Sci.* **2016**, 469, 310.
- [49] M. Nasrollahzadeh, S. M. Sajadi, M. Maham, *J. Mol. Catal. A* **2015**, 396, 297.
- [50] L. Chen, S. Rangan, J. Li, H. Jiang, Y. Li, *Green Chem.* **2014**, 16, 3978.
- [51] H. Alamgholiloo, S. Rostamnia, A. Hassankhani, J. Khalafy, M. M. Baradarani, G. Mahmoudi, X. Liu, *Appl. Organometal. Chem.* **2018**, 32, e4539.
- [52] S. Gao, Y. Huang, M. Cao, T.-f. Liu, R. Cao, *J. Mater. Chem.* **2011**, 21, 16467.
- [53] Y. K. Hwang, D. Y. Hong, J. S. Chang, S. H. Jhung, Y. K. Seo, J. Kim, A. Vimont, M. Daturi, C. Serre, G. Férey, *Angew. Chem.* **2008**, 120, 4212.
- [54] Y. K. Hwang, D. Y. Hong, J. S. Chang, S. H. Jhung, Y. K. Seo, J. Kim, A. Vimont, M. Daturi, C. Serre, G. Férey, *Angew. Chem. Int. Ed.* **2008**, 47, 4144.
- [55] L. Xue, Z. Lin, *Chem. Soc. Rev.* **2010**, 39, 1692.
- [56] P. Surawatanawong, M. B. Hall, *Organometallics* **2008**, 27, 6222.

SUPPORTING INFORMATION

Additional supporting information may be found online in the Supporting Information section at the end of this article.

How to cite this article: Alamgholiloo H, Rostamnia S, Noroozi Pesyan N. Extended architectures constructed of thiourea-modified SBA-15 nanoreactor: A versatile new support for the fabrication of palladium pre-catalyst. *Appl. Organometal. Chem.* 2020;e5452. <https://doi.org/10.1002/aoc.5452>